UNIVERSITEIT
AMSTERDAM

VU Research Portal

Proximity effects in the superconductor/heavy-fermion bilayer system Nb/CeCu6

Otop, A.; Boogaard, G. R.; Hendrikx, R. W. A.; Hesselberth, M. B. S.; Ciuhu, C.; Lodder, A.; Aarts, J.M.

Link to publication in VU Research Portal

Download date: 23. May. 2021

Proximity effects in the superconductor/heavy-fermion bilayer system $Nb/CeCu_6$

A. Otop[1,2], G. R. Boogaard[1](*), R. W. A. Hendrikx[1], M. B. S. Hesselberth[1], C. Ciuhu[3], A. Lodder[3] and J. Aarts[1]

[1] *Kamerlingh Onnes Laboratory, Leiden University*
P.O. Box 9504, 2300 RA Leiden, the Netherlands
[2] *Institut für Metallphysik und Nukleare Festkörperphysik*
Technische Universität Braunschweig - Mendelssohnstr. 3
38106 Braunschweig, Germany
[3] *Faculty of Sciences, Vrije Universiteit - De Boelelaan 1081*
NL-1081 HV Amsterdam, the Netherlands

Abstract. – We have investigated the proximity effect between a superconductor (Nb) and a "heavy-fermion" system ($CeCu_6$) by measuring critical temperatures T_c and parallel critical fields $H_{c2}^{\parallel}(T)$ of Nb films with varying thickness deposited on 75 nm thick films of $CeCu_6$, and comparing the results with the behavior of similar films deposited on the normal metal Cu. For Nb on $CeCu_6$, we find a strong decrease of T_c with decreasing Nb thickness and a finite critical thickness of the order of 10 nm. Also, dimensional crossovers in $H_{c2}^{\parallel}(T)$ are completely absent, in strong contrast with Nb/Cu. Analysis of the data by a proximity effect model based on the Takahashi-Tachiki theory shows that the data can be explained by taking into account both the high effective mass (or low electronic diffusion constant), *and* the large density of states at the Fermi energy which characterize the heavy-fermion metal.

Introduction. – When a superconductor (S) is brought into contact with a non-superconducting conductor (N), superconductivity leaks into that material by the proximity effect [1]. For the thermodynamic properties of the S/N bilayer such as the critical temperature T_c or the upper critical field H_{c2}, this can be modelled as a spatial variation of the superconducting pair density. The spatial variation mainly depends on the electron diffusion constants for the S- and the N-metal, on the transparency of the interface for electrons and Cooper pairs, and on the pair-breaking mechanisms on the N-side of the interface. Until now, two classes of N-materials have been investigated. The first is formed by simple metals such as Cu or Au, where the physics is mostly understood. Pairs are broken at finite temperatures by thermal fluctuations, leading to dephasing of the constituents of the induced Cooper pair. This is translated

---

(*) Present address: Department of Nanoscience, Delft University of Technology - Delft, the Netherlands.

into a temperature-dependent characteristic length over which superconducting correlations penetrate, the "normal-metal coherence length" ξ_{N}. Since $\xi_{\mathrm{N}} = \sqrt{(\hbar D_{\mathrm{N}})/(2\pi k_{\mathrm{B}} T)}$ (D_{N} is the diffusion constant of the N-metal, T is the temperature, the other symbols have their usual meaning), this length can become large at low temperatures. In the absence of other pair breakers (including the effects of localization), T_{c} of a bilayer with finite N-layer thickness d_{N} will be finite for all values of the S-layer thickness d_{S}. The other class of materials is formed by ferromagnets (F) such as Fe; pair breaking is due to the exchange interaction E_{ex} which acts on the spins of the Cooper pair. For strong magnets ($E_{\mathrm{ex}} \gg k_{\mathrm{B}} T_{\mathrm{c}}$) it results in a temperature-independent $\xi_{\mathrm{F}} = \sqrt{(\hbar D_{\mathrm{F}})/(2\pi E_{\mathrm{ex}})}$ with a characteristic value of only a few nanometers. In this case, in the regime of half-infinite F-layers ($d_{\mathrm{F}} \gg \xi_{\mathrm{F}}$), superconductivity is quenched at a finite value for d_{S}, called the critical thickness $d_{\mathrm{S}}^{\mathrm{cr}}$ [2–4].

Little attention has yet been paid to N-layers, where the electronic ground state is dominated by many-body correlations, such as in a heavy-fermion (HF) metal. Basically, HF metals consist of a lattice of atoms with localized (f-)electrons, where the magnetism is quenched by a coherent Kondo effect. This leads to a strong peak in the DOS near the Fermi energy with small energy width (for relevant reviews, see [5,6]). The consequences for the low-temperature physics can be phenomenologically described in terms of Landau Fermi liquid theory by a mass renormalization of the charge carriers. The ensuing large effective mass m^* can be directly observed in, e.g., the specific heat of the system, c_v, where the linear term $\gamma = c_v/T \propto m^*/m_{\mathrm{e}}$ (with m_{e} the bare electronic mass) can be up to two orders of magnitude larger than in normal metals. Since the magnetic moments are often not completely quenched, HF systems can also show magnetic order at low temperatures. For the proximity effect in an S/HF system, several scenarios are possible. In the spirit of the Fermi-liquid approach, the HF metal can be considered a normal metal with a large mass, or, equivalently, a low Fermi velocity and therefore a small diffusion constant. Also, additional pair breaking mechanisms may be present due to the strong electron-electron interactions or the residual moments. On the other hand, the interface transparency may be decreased due to the mismatch in Fermi velocities, which would shield the superconductor from the HF metal and counter the other two effects.

In order to investigate these questions, we have performed a comparative proximity effect study of the thin-film systems $\mathrm{Nb}/\mathrm{CeCu_6}$ and Nb/Cu. $\mathrm{CeCu_6}$ is a well-known HF system, with an extremely large value of $\gamma \approx 1.6\,\mathrm{J}/(\mathrm{mole\,K^2})$ [7] and no magnetic order down to the mK-regime, making it a good model system for this study. Nb/Cu is a much studied proximity system which shows one feature of particular interest, namely a Dimensional Crossover (DCO) from three-dimensional (3D) to two-dimensional (2D) behavior in the temperature dependence of the critical field parallel to the layers $H_{\mathrm{c2}}^{\parallel}$ [8,9]. The DCO occurs when the N-layer thickness becomes of the order of ξ_{N}, and can be modelled quite accurately. In particular, recent calculations by Ciuhu and Lodder based on the Takahashi-Tachiki theory for metallic multilayers [10], and including a finite interface resistance R_{B}, showed that quantitative agreement between theory and experiment can be found in the case of Nb/Cu for very reasonable values of the different parameters [11]. Here we present data on $T_{\mathrm{c}}(d_{\mathrm{S}})$ and $H_{\mathrm{c2}}^{\parallel}(T)$ for bilayers Nb/Cu and $\mathrm{Nb}/\mathrm{CeCu_6}$ and compare them with similar calculations. We show that the HF system can be treated as a normal metal, with *both* the low-diffusion constant (Fermi velocity) *and* the high DOS as necessary ingredients to explain the observed behavior.

Experimental. – Sets of $\mathrm{CeCu_6}$ films and bilayers of *sub*/$\mathrm{CeCu_6}$/Nb (*sub* denotes the substrate) were fabricated by DC-magnetron sputtering in an ultra-high-vacuum (UHV) system with a background pressure of the order of 5×10^{-10} mbar, and an Ar sputtering pressure of 2.5×10^{-3} mbar. Crystalline $\mathrm{CeCu_6}$ was grown as reported before [12], at a temperature of $350\,^{\circ}\mathrm{C}$, using Si-substrates with amorphous $\mathrm{Si_3N_4}$ buffer layers to prevent Cu diffusion at
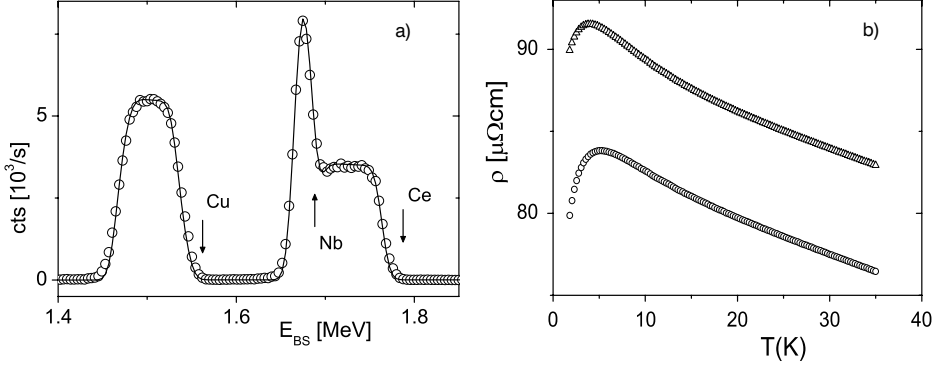
Fig. 1 – Materials characteristics of the CeCu$_6$ films. (a) RBS spectrum (number of counts *vs.* backscatter energy E_{BS}) taken with ^{4}He-ions of 2 MeV on a sample Si/Si$_3$N$_4$/(75 nm CeCu$_6$)/(15 nm Nb). The different elements are indicated. The thin smooth line is a fit to the measured curve. (b) Specific resistance as a function of temperature for single CeCu$_6$ films of 75 nm ($\circ$) and 100 nm ($\triangle$).

those temperatures. The Nb was deposited on top of the CeCu$_6$ after cooling the substrate holder with cold nitrogen gas to close to about room temperature. Composition, thickness and crystallinity of the films were determined by Rutherford BackScattering (RBS) measurements together with X-ray diffraction measurements at low and high angles. The RBS measurements show good agreement with the expected stoichiometry for CeCu$_6$ and no diffusion is found either of Ce or Cu into the substrate or of Nb into the CeCu$_6$. Figure 1a) shows part of the RBS spectrum for CeCu$_6$(75 nm)/Nb(15 nm) on a Si/Si$_3$N$_4$ substrate and a fit of the data without taking any diffusion into account. Bilayers and trilayers of *sub*/Cu/Nb and Cu/Nb/Cu were grown in a different UHV system with similar background pressure and sputtering conditions. In order to compare results, d_{Nb} in the trilayers was taken two times d_{Nb} in the bilayers, which yields equal conditions for the superconducting order parameter in the middle of the film (for the trilayer) and at the vacuum interface (for the bilayer).

Resistance measurements were performed in standard 4-point geometry on lithographically patterned samples with bridge widths of 200 μm and a distance of 1.2 mm between the voltage contacts. The electrical resistivity ρ_{CeCu_6} as a function of temperature for two single films is shown in fig. 1b) and behaves as reported before [12], with a clear maximum in $R(T)$ at $T_{max} \approx 5$ K, similar to what is found for bulk material [13], and a residual resistivity of the order of 80 $\mu\Omega$cm. We decided to use 75 nm thick CeCu$_6$ layers, which with $T_{max} = 4$ K suggest only little deviation from the bulk properties.

Results and discussion. – The dependence of T_c on d_{Nb} for the bilayer set *sub*/CeCu$_6$(75 nm)/Nb(d_{Nb}) is shown in fig. 2a) and compared to that of single Nb films, prepared in both UHV systems. For the Nb films a slight suppression is witnessed, usually found in the case of Nb, and caused by a mixture of different effects such as oxidation through the unprotected top layer, a small proximity effect with the substrate, and lifetime broadening due to growth disorder [14]. For the S/HF bilayers, the suppression is much stronger, with a critical thickness d_S^{cr} for onset of superconductivity reached around 12 nm. This would be equivalent to 24 nm in a trilayer configuration, and is of a similar magnitude as found in superconductor/ferromagnet systems such as V/Fe and Nb/Fe [3,15]. The result shows immediately that the interface does allow particle exchange, so the supposed huge Fermi velocity mismatch in the system of order 10^3 does not lead to a highly reflective interface. It also
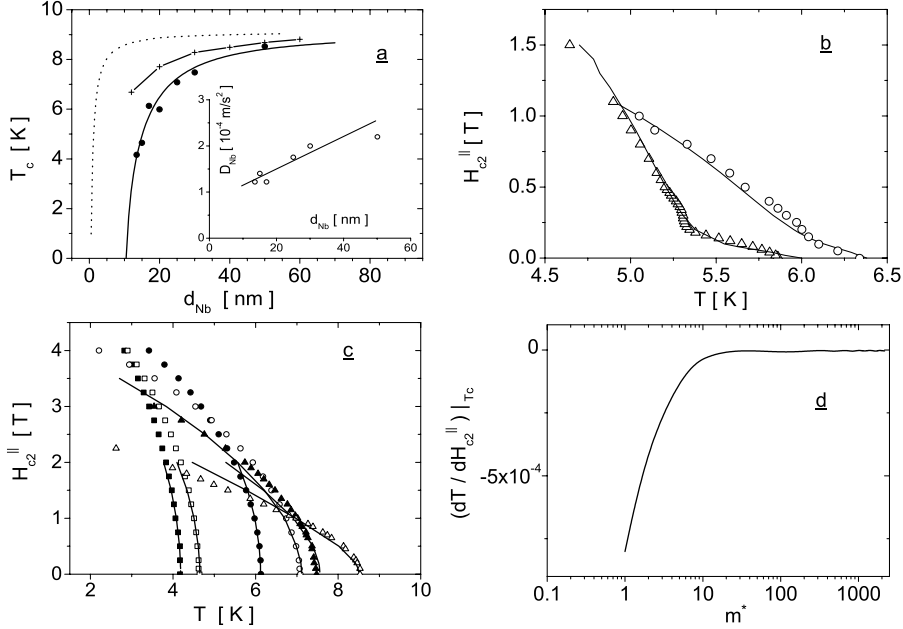
Fig. 2 – (a) T_c as a function of Nb thickness d_{Nb} for bilayers $sub/CeCu_6/Nb$ ($\bullet$) and single Nb films (+). The drawn line is a fit using the proximity effect model. The dotted line is a model calculation with $N_{CeCu_6} = N_{Cu}$. The inset shows the behavior of D_{Nb} as found from the fit. (b) Parallel critical field $H_{c2}^{\parallel}$ as a function of T for a bilayer $sub/Cu/Nb$ ($\triangle$ $d_{Nb} = 15\,nm$) and a trilayer Cu/Nb/Cu ($\circ$ $d_{Nb} = 30\,nm$). Drawn lines are model fits. (c) $H_{c2}^{\parallel}$ as a function of T for bilayers $sub/CeCu_6/Nb$ with thicknesses $d_{Nb} = 13.5\,nm$ (lowest T_c), $15\,nm$, $17\,nm$, $25\,nm$, $30\,nm$, $50\,nm$. Drawn lines are model fits. (d) Model calculation of the inverse slope of $H_{c2}^{\parallel}$ at T_c vs. the effective electron mass m^*.

shows that the coherence length in the HF-material ξ_{HF} must be small, leading to the strong suppression.

Another indication of behavior deviating from simple S/N systems comes from the parallel critical field $H_{c2}^{\parallel}(T)$. To demonstrate the difference, fig. 2b) shows $H_{c2}^{\parallel}(T)$ for a bilayer of $sub/Cu(75\,nm)/Nb(15\,nm)$ and a trilayer of Cu(75\,nm)/Nb(30\,nm)/Cu(75\,nm), to be compared to the data of the S/HF bilayers given in fig. 2c). Decreasing T near T_c, $H_{c2}^{\parallel}(T)$ is linear for the Nb/Cu samples, followed by a kink and $\sqrt{1 - T/T_c}$-like 2D behavior. The kink signals the well-known DCO [8,9], usually observed in multilayers, but also present in tri- and bilayers. In strong contrast, the S/HF bilayers do not show a DCO but only 2D behavior for all d_{Nb}. Qualitatively, this again indicates a small value for ξ_{HF}: the superconducting order parameter does not penetrate sufficiently far into the HF metal to yield a coupled system.

To make more quantitative statements, we analyzed the data by means of model calculations based on the Takahashi-Tachiki formalism. Details are given in ref. [11], but we reiterate the main elements in order to introduce the different parameters. The formalism solves the equation for the pair potential $\Delta(\boldsymbol{r})$ with a space-dependent coupling constant $V(\boldsymbol{r})$ for small Δ close to T_c:

$$\Delta(\boldsymbol{r}) = V(\boldsymbol{r})k_B T \sum_\omega \int \mathrm{d}^3\boldsymbol{r}' Q_\omega(\boldsymbol{r}, \boldsymbol{r}')\Delta(\boldsymbol{r}'), \tag{1}$$

in which Q_ω is an integration kernel still to be determined, $V(\boldsymbol{r})$ is the BCS coupling constant

Table I – *Values for the normal metal thickness d_N (in nm), the fitted values for the diffusion constants D_{Cu}, D_{CeCu_6}, D_{Nb} (in 10^{-4} m^2/s) and the interface resistance R_B (in 10^{-8} $\mu\Omega$cm^2) for the different samples discussed in the text.*

Metal	d_N	D_N	D_{Nb}	R_B
Cu (bi)	15	240	1.4	177
Cu (tri)	30	220	2.9	252
CeCu$_6$	13.5	0.15	1.2	324
	15	0.19	1.4	338
	17	0.11	1.2	350
	25	0.11	1.75	252
	30	0.11	2.	252
	50	0.11	2.2	324

and the other symbols have their usual meaning; the summation runs over the Matsubara frequencies. In the dirty limit, Q_ω can be shown to obey

$$\left[2|\omega| - \hbar D(\boldsymbol{r}) \left(\boldsymbol{\nabla} - \frac{2ie}{\hbar c} \boldsymbol{A}(\boldsymbol{r}) \right)^2 \right] Q_\omega \big(\boldsymbol{r}, \boldsymbol{r}'\big) = 2\pi N(\boldsymbol{r}) \delta\big(\boldsymbol{r} - \boldsymbol{r}'\big), \tag{2}$$

with $N(\boldsymbol{r})$ the DOS at the Fermi energy and $D(\boldsymbol{r})$ the diffusion constant. These equations are complemented with boundary conditions for Δ at the interface which parametrize a possible barrier encountered by the electrons through a boundary resistivity R_B. In the calculations we use fixed values for the density-of-states ratios $N_{Cu}/N_{Nb} = 0.16$ and $N_{CeCu_6}/N_{Nb} = 320$. The former value was also used in ref. [11] and derives from ref. [16]; the latter value is constructed from the former by the ratio $\gamma_{CeCu_6}/\gamma_{Cu} = 2000$. The value of $T_{c,Nb}$ was fixed at 9.2 K, except for the Nb/Cu bilayer with $d_{Nb} = 15$ nm, where it was 8.2 K. This reflects the fact that T_c for thin Nb-layers starts to decrease, as explained above. Fitted were the different diffusion constants D_N and boundary resistances R_B. The results of the fits for the critical field data are shown in fig. 2 as solid lines. The parameter values are given in table I. For the two Nb/Cu samples, the fitted values are in very reasonable agreement with the numbers found by fitting the data of Chun *et al.* [9, 11]. The values for D_{Nb} are roughly equal, the values for D_{Cu} are slightly higher, which probably reflects the difference in preparation conditions, and also the values for R_B are very similar [17]. For the Nb/CeCu$_6$ samples it can be noted that D_{Nb} increases slowly and more or less linearly with increasing d_{Nb}; using this linear variation, which is plotted in the inset of fig. 2a), and values of $D_{CeCu_6} = 0.1 \times 10^{-4}$ m^2 s^{-1}, $R_B = 324 \times 10^{-8}$ $\mu\Omega$cm^2, we calculated the behavior of $T_c(d_S)$ as a consistency check. The agreement, shown in fig. 2a), is equally satisfactory. The most interesting values from the fits are of course those for D_{CeCu_6}, which are much lower than those for Cu. Assuming a Fermi velocity of the order of 10^3 m/s, a value for D_{CeCu_6} of 0.1×10^{-4} m^2/s yields a mean free path l_e of 3 nm, which is not surprising in view of the strongly granular nature of the films. Still, a low value for D_N by itself does not necessarily reflect the heavy-fermion character: if CeCu$_6$ is taken as a Cu matrix strongly diluted by a small amount of Ce atoms, with a mean free path of the order of the interatomic distance, D would also be very small, of order 10^{-4} m/s. However, as we show now, just a low value for D_N cannot describe the measurements. To demonstrate this, we calculated $T_c(d_S)$ for Nb/CeCu$_6$ with the parameters given above, but with the DOS ratio for Nb/Cu, thereby mimicking a very dirty but otherwise standard N-metal. The result, shown in fig. 2a) as dotted line, shows that T_c now drops at much lower

d_{Nb}. This can be understood by realizing that the low-diffusion constant inhibits penetration of Cooper pairs in the N-metal and therefore also inhibits pair breaking, leading to a smaller amount of suppression of T_c. What makes the difference is the high DOS value for CeCu$_6$: the large number of available states works as a sink for Cooper pairs which counteracts the low-diffusion constant. Our major conclusion is therefore that both the low D_N *and* the high N_N are necessary ingredients in the description of the data. This leads to the question what the effective mass needs to be in order to suppress the DCO which is so characteristic for an S/N system. For this we calculated values for $dT/dH_{c2}^{\parallel}|_{T_c}$, the inverse parallel critical field slope at T_c, as a function of the effective mass m^*/m_e (m_e being the bare electron mass) as used in the free-electron expressions for $N_N = \frac{m^* k_F}{\hbar^2 \pi^2}$ and $D_N = \frac{k_F l_e}{3 m^*}$, with k_F the Fermi wave vector. As shown in fig. 2d), low values for m^* yield a finite value for the inverse slope, signifying 3D behavior and therefore a DCO, which goes to 0 around $m^* = 10$, meaning that the DCO has disappeared and 2D behavior has set in. Clearly, CeCu$_6$ is well into this regime.

Finally, we come back to the difference in proximity effects between F-, and HF-metals. Using the expression for ξ_N given in the introduction at a typical value of $T = 5$ K and with the fitted values for D_{CeCu_6}, we find $\xi_{CeCu_6} \approx 1.5$ nm. This is very similar to values found for strong ferromagnets, but the physics of the strong suppression of superconductivity which is found both in the F- and HF-systems is different. In the F-case, the small value of ξ_F derives from the large pair breaker (E_{ex}), in the HF-case from the small D_N. As shown in fig. 2a, a low value for D_N does not yield strong suppression of superconductivity; the suppression is actually due to the high value for N_N. This emphasizes once more that the basic proximity-effect parameter is not $\xi_{F,HF}$ but rather $\gamma = (\rho_S \xi_S)/(\rho_X \xi_X)$ with X = F, HF [3,18]. Since $\rho_X \propto (N_X D_X)^{-1}$ and $\xi_X \propto \sqrt{D_X}$, it can easily be seen that for the F-system γ is large due to E_{ex}, and for the HF-system γ is large due to N_{CeCu_6}. For the HF-system, an extra pair breaker is not needed in the description.

$$* * *$$

REFERENCES

[1] DE GENNES P. G., *Rev. Mod. Phys.*, **36** (1964) 225.
[2] MÜHGE TH. M., GARIF'YANOV N. N., GORYUNOV YU. V., KHALIULLIN G. G., TAGIROV L. R., WESTERHOLT K., GARIFULLIN I. A. and ZABEL H., *Phys. Rev. Lett.*, **77** (1996) 1857.
[3] AARTS J., GEERS J. M. E., BRÜCK E., GOLUBOV A. A. and COEHOORN R., *Phys. Rev. B*, **56** (1997) 2779.
[4] For the case $d_F \leq \xi_F$, the behavior of $T_c(d_S)$ is more complicated due to the fact that an inhomogeneous order parameter is induced in the ferromagnet. See, for instance, GARIFULLIN I. A. *et al.*, *Phys. Rev. B*, **66** (2002) 020505(R).
[5] HEWSON A. C., in *The Kondo Problem to Heavy Fermions, Cambridge Studies in Magnetism*, part 2 (Cambridge University Press) 1993.
[6] NIEUWENHUYS G. J., in *Handbook of Magnetic Materials*, edited by BUSCHOW K. H. J., Vol. **9** (Elsevier Science) 1995, p. 1.
[7] SCHLAGER H. G., SCHRÖDER A., WELSCH M. and VON LÖHNEISEN H., *J. Low Temp. Phys.*, **90** (1993) 181.
[8] BANERJEE I. and SCHULER I. K., *J. Low Temp. Phys.*, **54** (1984) 501.

[9] Chun C. S. L., Zheng G.-G., Vincent J. L. and Schuller I. K., *Phys. Rev. B*, **29** (1984) 4915.

[10] Takahashi S. and Tachiki M., *Phys. Rev. B*, **33** (1986) 4620.

[11] Ciuhu C. and Lodder A., *Phys. Rev. B*, **64** (2001) 224526.

[12] Groten D., van Baarle G. J. C., Aarts J., Nieuwenhuys G. J. and Mydosh J. A., *Phys. Rev. B*, **64** (2001) 144425.

[13] Amato A., Jaccard D. and Walker E., *Solid State Commun.*, **58** (1985) 507.

[14] Park S. I. and Geballe T. H., *Physica B*, **135** (1985) 108.

[15] Geers J. M. E., Hesselberth M. B. E., Aarts J. and Golubov A. A., *Phys. Rev. B*, **64** (2001) 094506.

[16] Banerjee I., Yang Q. S., Falco C. M. and Schuller I. K., *Solid State Commun.*, **41** (1982) 805.

[17] The values for R_B given in ref. [11] are quoted in units $\mu\Omega$cm and were obtained by somewhat arbitrarily multiplying the fitted value for R_B by a sheet thickness of 10 nm. A value such as $3.17\,\mu\Omega$cm in ref. [11] therefore corresponds to $317 \cdot 10^{-8}\,\mu\Omega$cm^2 in the present paper.

[18] Golubov A. A., *Proc. SPIE*, **2157** (1994) 353.